# Design Rules for Additive Manufacture

I. Gibson, G. Goenka, R Narasimhan, N Bhat

## Introduction

As Rapid Prototyping (RP) has evolved to become Additive Manufacture (AM) it has become possible to exploit the effects of the layer-based approach to fabrication so that parts can become easier to build and with greater functionality. Initially parts made in a manner that could not be manufactured further using conventional processes were considered merely as a novelty to RP machine users rather than of any wider benefit. With improvements in the technology and increasing demand for more complex geometry products, AM is coming into its own. As a result, we are now able to manufacture parts that have interlocking features, overlapping and mechanistic properties as well as us not having to worry about constraints like draft angles and overhanging features.

However, this does not mean we can completely ignore manufacturing constraints. More that we have to concern ourselves with a different set of constraints. AM technologies are limited according to the following (1): -

- Speed of build
- Accuracy
- Surface geometry
- Tolerances
- Wall thickness and feature size
- Material properties
- Range of materials

These have always been an issue; it's just that now improvements have now gotten to the stage where parts are acceptable for final application. We must therefore concern ourselves with a new set of design rules that allow us to understand how the technology can be best applied to the advantage of the creator of the new products.

## Background

It has always been known that parts could be made using (what was then known as) RP that could not be easily manufactured in a conventional manner. This was indeed what made it easier to use the technology in the early stages of the product development process. There was no need to consider draft angles or seriously worry about overhangs, radiuses, ribs, etc. that may affect the quality of a final moulded part, thus allowing the designer to focus on the form and function of the design. However, it was always considered that the final product would be made using conventional processes because the first RP machines were expensive, inaccurate and slow to build a single part from materials that were also expensive, had poor mechanical properties and suffered from long-term degradation and distortion effects.

Mainly incremental improvements in the technology have focused on lowering machine costs whilst increasing build speeds and accuracies. Parallel improvements in materials have resulted

in a wider range with superior properties that are consequently suited to a much wider range of applications. Many of these applications are now destined for final use rather than just earlier stages of the product development process. Furthermore, it is now possible for example to include integral gears and cams, mechanical and living hinges, snap fasteners and even fully interlocking meshes like chain mail into a design and in a single manufacturing stage with AM technology (like the examples shown in figure 1). Metal systems have also become a reality in recent years to enhance this rich arsenal of tools that can tie design to manufacture in an unprecedented manner.

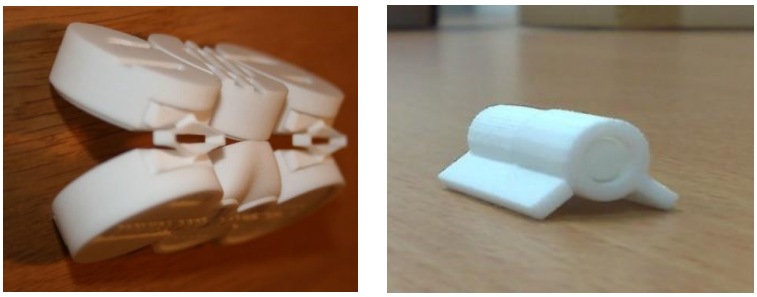

**Figure 1: AM feature samples (Courtesy EOS and Shapeways)**

It is only now that designers are waking up to the possibilities this technology can provide. Companies like Shapeways (2), Freedom of Creation (3) and MGX (4) are at the forefront of this wave, providing innovative designs that exploit the capabilities of AM technology. However, these companies are also exploiting their position in the marketplace, having extensive understanding and experience of the technologies. There are currently very few tools that support the design process with focus on AM technologies. Probably the most extensive research has been undertaken by Campbell (5), who has focused on the development of a database that indicates to the designer what different features can be included into a new product. This will enable the designer to exploit new design possibilities but falls short of quantifying the outcomes of any new design proposals. Earlier work by Campbell and by Choi (6) tried to simulate AM technology so that users and designers can understand how parts might be affected by the layer-based technology and the orientation inside the machine, for example, but this was more analytical and did not provide any initial rules for such a design. EOS carried out a study that proposed a variety of living hinge designs based on a basic set of material properties (7). This study can help designers understand how different designs might function but it is still somewhat difficult to understand how to fine-tune a design using the proposed hinge designs.

When designing parts that will finally be built using AM technology, we are not talking about eliminating process constraints but incorporating a new set of constraints. Definitely these constraints are more relaxed in terms of overall functionality of part, but we must still understand the process and materials fully in order to get the best out of the resulting parts and to avoid mistakes. The purpose of this study is to try and understand the material issues in parts made using AM so that we may be able to generate a set of quantifiable rules that can allow designers to exploit them. The ultimate aim of this work is to provide sets of rules that can allow reliable designs that also stretch the capabilities of the processes. There are numerous AM technologies available, with new processes and machines being introduced to the market at regular intervals. Existing machines are also extended by the introduction of new materials and innovative post-

processing techniques. It is therefore important to focus on design rules that are flexible enough to accommodate these technological developments, so that we can: -

- Choose the correct process and materials from what is available
- Define lower limits that can ensure a design feature will work from the chosen machine parameters
- Determine whether a specified design might work once it has been fabricated

Our initial study was to investigate whether we can apply a more precise set of rules to living hinge design. This study quickly moved on to a more detailed understanding of the living hinge concept so that it was possible to develop and validate numerical models that exploited in the basic principles of viscoelasticity in the materials concerned. The rest of this paper will therefore discuss the basic mechanical properties before going on to describe a series of experiments that support a numerical model of a viscoelastic feature. We will then proceed to a discussion on how this work can assist in providing support for product designers who want to use AM technology.

## Study into elastomeric properties of AM materials

*Initial Analysis:* Elastomeric properties can be included in a wide range of applications to produce living hinges, snap fits, seals, shock-absorbers etc. While different features ideally require a unique set of material properties, most of the features which make use of the elastomeric properties require the material to able to bend, stretch or compress. The objective of the study was to understand the kinematics of the bending mechanism which could be used in features like elastic hinges and find a suitable AM material which would be able to undergo the maximum amount of bending before failure by yield or fracture and be able to withstand a small amount of load. The best material is the one which for given ligament dimensions bends to the smallest radius without yielding or failing (8). When a ligament of thickness 2t is bent elastically to a radius R, the surface strain is

$$\varepsilon = \frac{t}{R}$$

Assuming that the bending is initially elastic, the maximum stress is

$$\sigma = E\frac{t}{R}$$

This must not exceed the yield or failure strength $\sigma_f$. Thus the radius to which the feature can be bent without damage is

$$R \geq t\left(\frac{E}{\sigma_f}\right)$$

The best material is the one that can be bent to the smallest radius, that is, the one with the greatest value of the index

$$M_1 = \frac{\sigma_f}{E}$$

It should also be able to withstand a certain amount of axial load (F). Assuming that w is the width and t is the thickness, the tensile stress in the feature should be

$$\sigma_f \geq \frac{F}{tw}$$

Substituting t in the earlier equation,

$$R \leq \frac{F}{w}\left(\frac{E}{{\sigma_f}^2}\right)$$

This gives the second index which should be optimized

$$M_2 = \frac{{\sigma_f}^2}{E}$$

The mechanical properties of some of the important AM processes were collected either through published data or from company representatives and compared using the two material indexes discussed before. The further in the upper right hand corner of the graph a dot is, the higher are the values of the 2 indexes and the better are the elastomeric properties of the material. The AM materials have been compared to polyethylenes (PE) and polypropelene (PP) which are the conventional types of plastics used in features which require elastomeric properties.

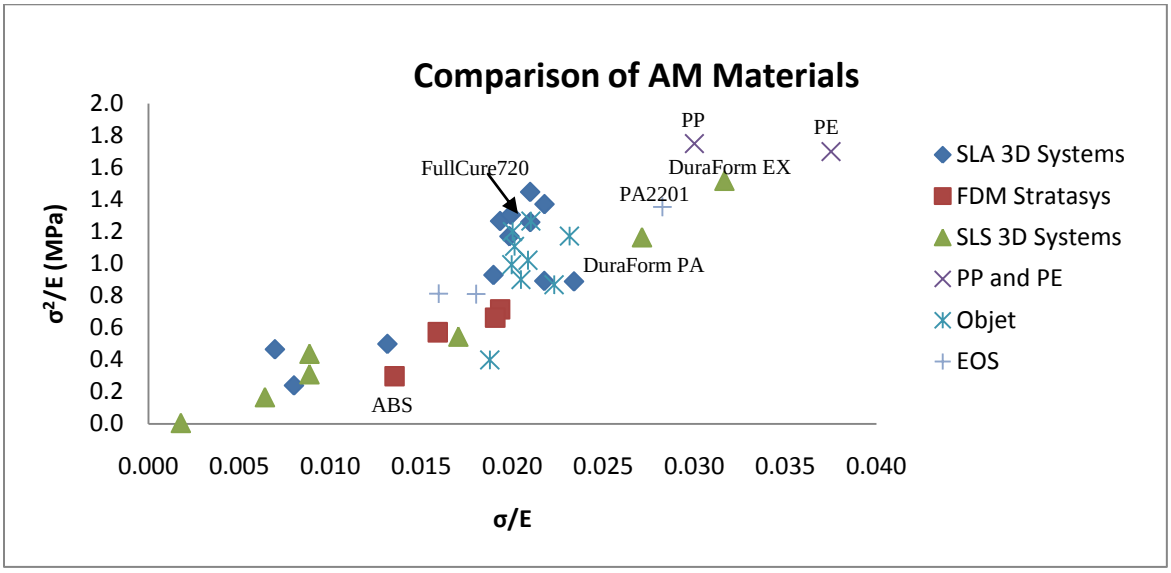


**Figure 2: Comparison of AM Materials**

It is noted from Figure 2 that even though PE and PP have the best elastomeric properties, some of the AM materials like Duraform EX from 3D Systems and PA2201 from EOS exhibit good elastomeric properties in terms of the 2 indexes chosen. It should also be noted that there are other factors like feature design and molecular orientation which also play a role in the final elastomeric properties of the part have been ignored in this study. For example, some of the

critical properties of PP can be improved by enhancing orientation through optimization of the melt temperature and fill speed in injection molding (9).

*Experimental analysis of elastomeric properties:* The Objet Eden 350 machine which uses the PolyJet Matrix 3D Printing technique was chosen for the study due to availability. Photopolymers are deposited in 0.0006 in. layers (1) by the print-head which are then cured by ultra-violet light immediately producing fully cured models without the need for post-curing. The support material, which is also a photopolymer, is removed by washing it away with pressurized water in a secondary operation. The Eden machines can only print one material at a time but the Connex machines provide multi-material capability.

FullCure 720 was chosen as the material for the investigation. It is a translucent acrylic based photopolymer material developed for Objet PolyJet-based 3D Printers. It is relatively rigid compared to DurusWhite FullCure 430 and is conventionally used to build rigid models where internal details are required (10). The material does not require any subsequent machining, has a high elongation at break and good flexural toughness (11). Palli et al (12) used FullCure 720 to successfully build integrated robotic fingers using pin joints which showed very good reliability and did not fail after one hundred thousand working cycles.

Studies have shown that photopolymers exhibit changes in mechanical properties with ageing and exposure to sunlight. This may be caused by the reaction of the radicals in the occluded sites with diffused oxygen or another reactive species (1). For the purpose of this study all the specimens were fabricated together. They were stored together for 10 days at room temperature and then tested together to offset the aging effects. There is some inherent anisotropy in the parts fabricated using the PolyJet process which may be due to layer-wise nature of the process. The specimens were fabricated in the same orientation to avoid any differences due to orientation.

In order to fully understand the elastomeric properties of a material and, it is imperative to have the full stress-strain curve of the material which was not publicly available for FullCure 720. As a result, compression tests were carried out following the ASTM D695-02 Standard Test Method for Compressive Properties of Rigid Plastics. Cylindrical specimens of diameter 12.7 mm (0.5 in) and length 25.4 mm (1 in) were prepared and tested using an INSTRON AG-25TB uni-axial tester (Figure 3) with a 25 kN load cell at a very low strain rate of $1.3 \times 10^{-3}$ $s^{-1}$. The effect of friction on the top and bottom surfaces of the specimen was reduced by applying a lubricant.

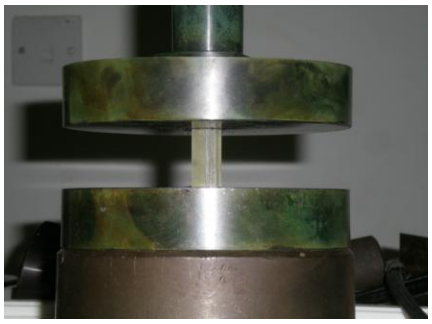

**Figure 3: Compression test**

The tests give a consistent set of results as shown in Figure 4.

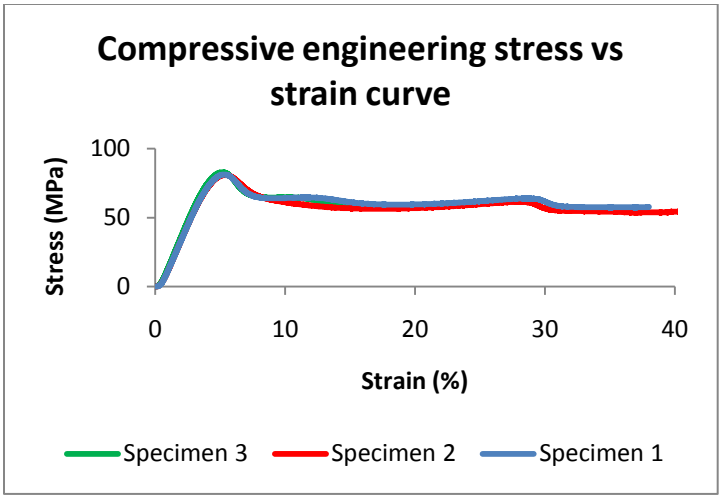


Figure 4: Compressive engineering stress vs strain curve

The material properties were calculated from the stress-strain curves obtained from the compression tests. After compensating for the toe region, stresses $\sigma_1$and $\sigma_2$ corresponding to the strain values $\varepsilon_1$= .0005 and $\varepsilon_2$= .05 were recorded (11) and the Young's modulus was calculated using the relation:

$$E = \frac{\sigma_2 - \sigma_1}{\varepsilon_2 - \varepsilon_1}$$

The Young's modulus was calculated to be 1700 MPa. It is noted that the stress-strain curve in Figure 5 exhibits a reversal of curvature indicating a softening phase over small strains followed by a hardening phase for larger strains.

Living hinges were identified as the feature to be used to study the bending phenomenon since the critical aspect in the functioning of living hinges is the material property unlike other structures gears and mechanical hinges which depend on process related properties like clearances and tolerances. The three main characteristics of the living hinge design are the recess (l) the thickness (2t) and length ($L_1$) of the neck region. These dimensions are illustrated in Figure 5.

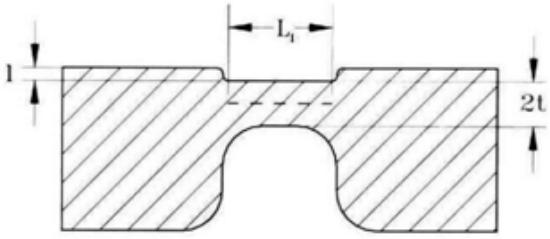


Figure 5: Living hinge dimensions

Specimens with different thicknesses of the neck region were fabricated to study their effects on the bending. A jig was developed which could be used along with a tensile micro-testing machine to bend the living hinges and record the force vs vertical displacement. It is better to use a torsion testing machine instead of a uni-axial tensile tester as one can achieve 180 degrees of

rotation through circular rotation. Unfortunately the standard torsion machine was not sensitive enough to correctly record the torque on the specimens and a micro-torsion machine was not available as a result of which the tests were carried out on the tensile micro-tester which was able to achieve a 45 degrees bending as shown in Figure 6.

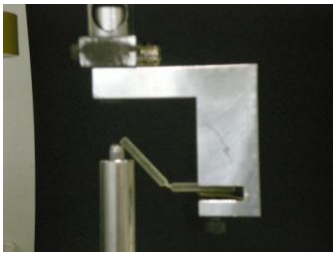

Figure 6: 45 degrees bending test of a living hinge

The dimensions of the test specimens were measured using the Mitutoyo digital caliper with the measurement range 0-150/0.01 mm. The average thicknesses (2t) of the specimen were 0.37 mm, 0.52 mm and 0.70 mm with standard deviation of 0.047, 0.039 and 0.028 respectively. The hinge length ($L_1$) was maintained constant at 3 mm with standard deviation of 0.016. The top recess (l) was also maintained constant at 0.40 mm. The height of the specimens was 2.30 mm while the breadth was 3.70 mm. A summary of the results of the tests is shown in Figure 7.

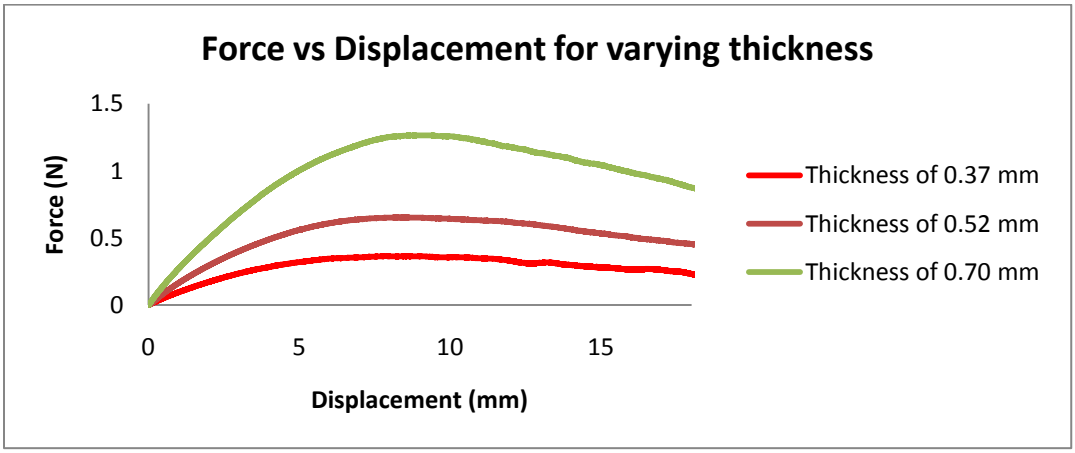


Figure 7: Force vs Displacement for varying thickness

As expected, the force required to bend the specimen increases as the thickness of the neck region increases. There is a decrease in the force once it has attained a peak value which could be attributed to the yielding and the resulting softening of the material. It could also be due to geometrical softening occurring due to necking in the hinge region.

## Finite Element Analysis of elastomeric materials

The objective of this part of the study was to develop a general Finite Element Analysis (FEA) model taking living hinges as an example which could be used to model different features which make use of the elastomeric properties of FullCure 720 or similar materials. The study

investigated the high deformation which occurs during the bending of a feature and examined the ability of FEA to predict the feature behavior by obtaining simulation results from a model that undergoes high element distortion. The analysis included the modeling of the geometry and boundary conditions replicating the experiment described earlier, the material properties obtained from the compression tests and structured mesh elements to calculate the contact forces which were compared to the results obtained from the experiments. Abaqus/Standard was chosen for the study after examining the large deformation capabilities of various FEA software packages.

The tests involved high strains and consequent material yielding which meant that an elastic-plastic model would be needed instead of a simple elasticity model. Since the compressive yield stress for FullCure 720 is 1.4 times higher than the tensile yield stress (10) indicating pressure-sensitive yielding (13), it was not possible to simulate the test using von Mises plasticity (14). While heterogeneous deformation is closely approximated by Mohr-Coulomb or modified Tresca criterion, the Drucker-Pragar yield criterion is suitable for polymers which undergo homogenous deformation (15). Even though the PolyJet process exhibits a small amount of anisotropy due to the layer-wise fabrication process, the anisotropy is small as compared to other processes and not well documented. Thus FullCure 720 was assumed to be strain-rate independent and undergo homogenous deformation and the original linear Drucker Pragar model with a symmetric stiffness matrix was used with $\sigma^c/\sigma^t$ as 1.4 in conjunction with the linear elastic model.

The angle of friction is given by: (16)

$$\tan\beta = \frac{3(\alpha - \frac{1}{K})}{\alpha + 1}$$

where $\alpha = \sigma^c/\sigma^t$. $\beta$ was calculated to be 26.5°.

The boundary conditions as shown in Figure 8 and 9 were defined to closely resemble the experiment conditions. A part right-hand side was constrained so it could not move in the x and y direction neither rotate about the z axis (referred to as ZASYMM constraint in Abaqus) to replicate the clamping mechanism used in the experiment where a screw pressed on the feature to prevent it from moving. A rigid analytical body was used to model the load pin which was made out of steel as the stiffness of steel is much higher than that of FullCure 720. The rigid body was constrained in the directions except translation along the y axis. As the load pin moved up along the y axis it pushed the feature thus bending it.

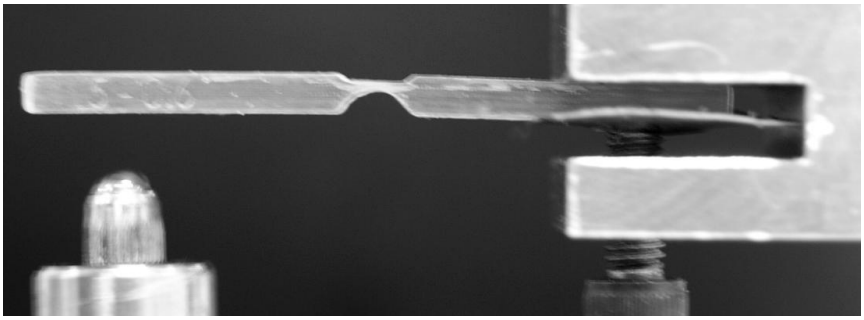

**Figure 8: Boundary conditions during the experiment**


Figure 9: Boundary conditions in the FE model

The Poisson's ratio is taken to be 0.3 as published by Vesenjak et al (17). Since Abaqus accepts only true stress-strain curves, the true stress and true strain were calculated from the engineering stress-strain curve using the relations:

$$\varepsilon_t = \ln(1 + \varepsilon_e)$$

$$\sigma_t = \sigma_e(1 + \varepsilon)$$

The subscripts t and e refer to true and engineering respectively. The model was unable to provide converging results for the softening phase in the stress-strain curve. Since the objective of the study was to model the feature behaviour at large deformations and the softening takes place over a relatively small region, the piecewise power law hardening law was used to approximate the stress-strain curve in order to get convergent solutions. Using Eqns:

$$\frac{\varepsilon^p}{\varepsilon_y} = \begin{cases} 0 & \sigma \leq \sigma_y \\ \left(\frac{\sigma}{\sigma_y}\right)^n & \sigma > \sigma_y \end{cases}$$

where $\varepsilon^p = \varepsilon - \frac{\sigma_y}{E}$, $\varepsilon_y$is the yield strain, $\sigma_y$is the yield stress and n is a constant which is assumed to be 50. The resulting approximation is shown in Figure 10.

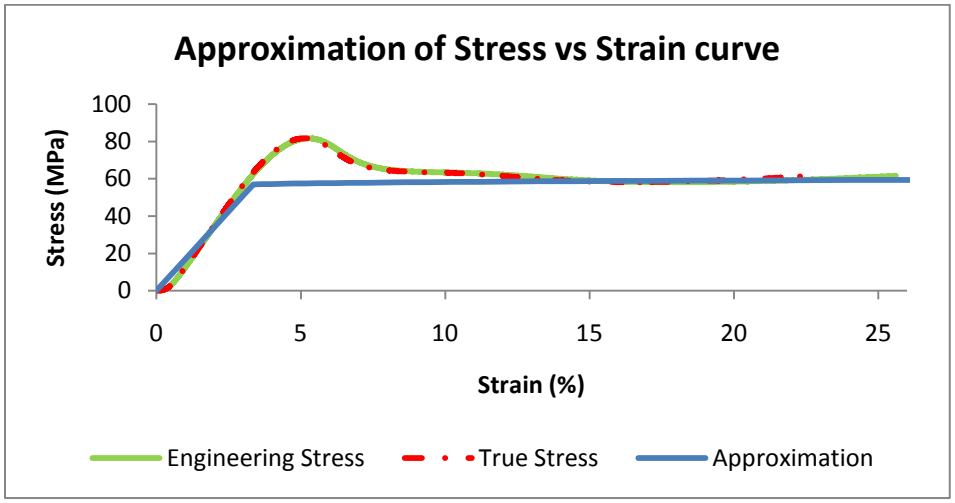


Figure 10: Approximation of Stress vs Strain curve

Since the feature modeled has a constant geometry through-out the cross-section, a two-dimensional model was initially used in order to reduce the solver time. Simulations were carried for both plane stress (referred to as CPS4 in Abaqus) and plane strain (referred to as CPE4H in Abaqus) elements but the results were not accurate. While the simulations with the plane stress element type gave the correctly predicted the peak force value, there was excessive local distortion in the neck region which led to unloading in the rest of the feature. On the other hand the simulations with the plane strain element type significantly overestimated the peak force value. Consequently a three-dimensional model was developed with 5796 eight-noded linear brick, hybrid elements (referred to as C3D8H in Abaqus). Analysis was initially carried out using reduced integration but it led to hour-glass formation and consequently hybrid formulation was adopted. The mesh was well refined near the region where the bending takes place with 75 nodes over a 3 mm region. The contact between the load-pin and the specimen was modeled using a penalty friction formulation with a frictional coefficient of 0.2 (18).

The results obtained from the experiments were compared against the finite element analyses using the output variable CFN signifying the total force due to contact pressure in Abaqus. Figure 11 shows the comparison between the specimens of average thickness 0.37 mm and the corresponding FE results while Figure 12 shows the comparison between the specimens of average thickness 0.70 mm and the corresponding FE results. It is noted that while the results agree closely for low strains, there is a slight divergence between the curves for large strains. This may have been due to the piece-wise power law approximation for large strains and also the predomination of non-linear visco-elasticity at higher strains leading to a decreased Young's modulus (19).

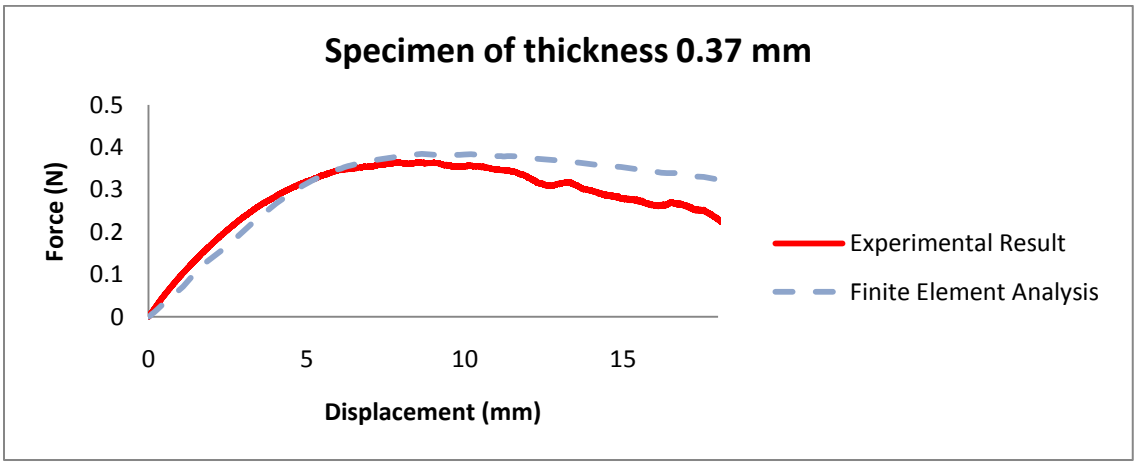


**Figure 11: Comparison between experiment and FE results for thickness of 0.37 mm**

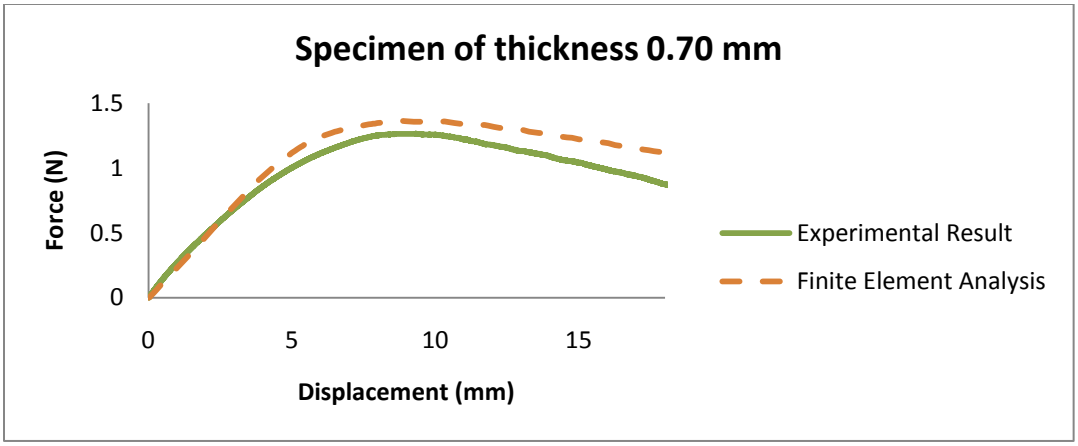


Figure 12: Comparison between experiment and FE results for thickness of 0.70 mm

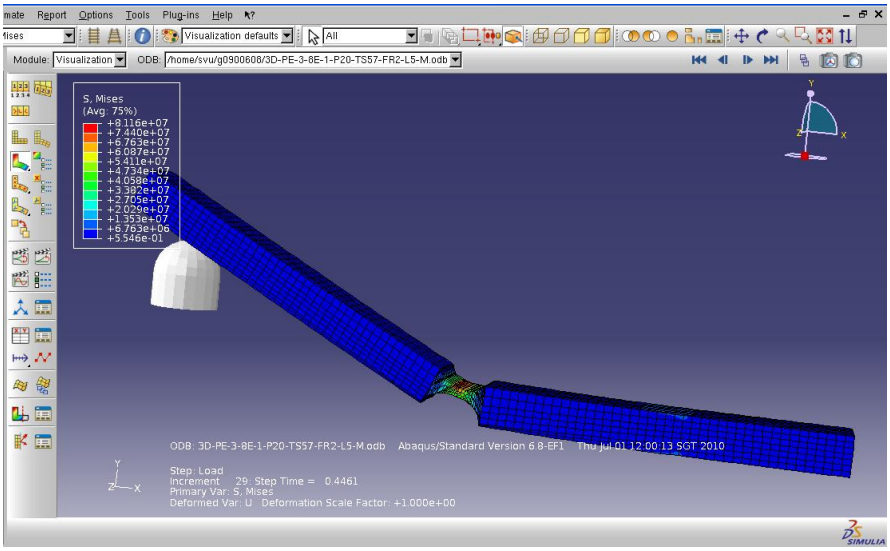


Figure 13: Screenshot of the FE model on Abaqus

## Discussion and Conclusions

We appear to have a good FE model that approximates and correlates well with the experimentation. The unloading phase which involves the visco-elastic phase could be investigated and modeled in the future. Moreover, the modeling of material softening as well as crack propagation and fatigue could lead to better prediction of failure.

Based on the initial analysis with the material indexes discussed earlier, FullCure 720 looked to be a good candidate for the fabrication of living hinges. However more precise models indicated problems. FullCure 720 does exhibit elastomeric properties but not strong enough to withstand heavy use. Further studies will investigate other materials and applications.

## Bibliography


1. **I. Gibson, D. W. Rosen, B. Stucker.** Additive Manufacturing Technologies, Springer , 2010.

2. *Shapeways* . [Online] [Cited: July 7, 2010.] www.shapeways.com.

3. Freedom of Creation . [Online] [Cited: July 7, 2010.] www.freedomofcreation.com.

4. *MGX.* [Online] [Cited: July 7, 2010.] www.materialise.com/MGX.

5. *Implications on Deisgn of rapid manufacturing.* **R Hague, I Campbell and P Dickens**, Journal of Mechanical Engineering Science, 2003.

6. *A versatile virtual prototyping system for rapid product development.* **H.H. Cheung, S.H. Choi**, Computers in Industry, 2008, Vol. 59.

7. **Nora González, Franz-Josef Kerl.** *Deisgn study: living hinges* . 2008.

8. **Ashby, MF.** *Materials Selection in Mechanical Design.*

9. *Pastic Integral Hinges: Design, Precessing, and Failure Analysis* . **Elleithy, Rabey H.** Ohio, Society of Plastics Engineers, 2007 .

10. FullCure 720 Transparent Materials.*Objet Geometries* . [Online] [Cited: July 8, 2010.] http://www.objet.com/Materials/FullCure720_Transparent/.

11. *Experimental analysis of properties of materials for rapid protoyping* . **Ana Pilipović, Pero Raos, Mladen Šercer** , Springer, 2007.

12. *Integrated Mechatronic Design for a New Generation of Robotic Hands* . **G. Berselli, G. Borghesan, M. Brandi, C. Melchiorri, C. Natale, G.Palli, S. Pirozzi, G. Vassura**, 2009.

13. *The plastic flow of isotropic polymers* . **P. B. Bowden, J.A. Jukes,** Journal of Material Science, 1972.

14. *Material behavior of polymers under impact loading* . **P.A. Du Bois, S. Kollong, M. Koesters, T. Frank**, International Journal of Impact Engineering , 2005.

15. *Characterisation of Pressure-sensitive yielding in polymers* . **P. Bardia, R. Narasimhan**, Strain, Blackwell Publishing Ltd, 2006.

16. *Abaqus 6.8 Documentation.*

17. *Computational Modelling of Closed- and Open-Cell Cellular Structures with Fillers.* **M. Vesenjak, A. Ochsner, Z. Ren.**

18. *Static friction coefficient of some plastics against steel and aluminum under different contact conditions.* **Benabdallah, Habib S**, Tribology International, Elsevier , 2006.

19. *A viscoelastic-viscoplastic constituive model for glass polymers.* **Geoffrey J. Frank, Robert A. Brockman**, International Journal of Solids and Structures, 1998.